

Stochastic Coherence in Coupled Map Lattices

Manojit Roy^a and R. E. Amritkar^b

^a*Department of Physics, University of Pune, Pune 411007, India*

^b*Physical Research Laboratory, Navrangpura, Ahmedabad 380009, India*

Abstract

We report in details the observations of *structures* in coupled map lattice during its chaotic evolution, both in one and two dimension, driven by identical noise on each site (by a structure we mean a group of neighboring lattice-sites for whom values of dynamical variable follow certain prespecified pattern). It is observed that the number of these structures decays with their size following a *power-law*, for a given noise-strength. The number of structures decays with their lifetime following a stretched exponential. We have seen an interesting phenomenon, which we call *stochastic coherence*, in which the average length as well as the average lifetime of these structures exhibit *bell-shaped* maxima for some intermediate range of noise-strength values. Similar features have also been observed for ‘spatio-temporal structures’.

Keywords: Chaos; noise; coupled map lattice.

I. INTRODUCTION

Over years coupled map lattice (CML) has become a very popular model to study a host of physical phenomena involving systems with spatial dimension [1–13]. In particular, CML exhibits a variety of spatio-temporal patterns and structures and has been extensively used, with varying degree of success, to model similar features in experimental systems such as Rayleigh–Bénard convection, Taylor–Couette flow, B–Z reaction etc. [1,2,5,6,14]. One of the challenging problems is to understand the formation of structures, localized in both space and time, in turbulent fluid [15–17]. Recently lot of attention has been devoted to the role of fluctuations in onset, selection and evolution of such patterns and structures [18–26]. An interesting and counterintuitive observation is that the presence of noise can help sustain structures which otherwise would have been absent in an evolving dynamical system.

In this paper we present the detailed account of a novel phenomenon that we have recently observed [27] in the dynamics of structures in a chaotically evolving CML, in one and two dimension, driven by identical noise. We call a *structure* as a group of neighboring sites whose variable-values follow certain prespecified spatial pattern. As the lattice evolves under the influence of noise, the number of these structures exhibits *power-law decay* with size of the structure for a given noise-strength, with an exponent which is a function of noise-strength. It is observed that average size of these structures, plotted against noise-strength, shows a bell-shaped curve with a characteristic peak. Similar features have been noted for the ‘spatio-temporal structures’ also (by this we mean the cluster of sites which remain in a structure as it evolves in time). Average lifetime of these structures also exhibit a maximum within same range of noise values. The behaviors remain essentially the same in two dimensional CML as well. We call this new phenomenon *stochastic coherence*.

II. THE SYSTEM

We first consider a one dimensional CML with the dynamics

$$x_{t+1}(i) = (1 - \varepsilon)F(x_t(i)) + \frac{\varepsilon}{2}[F(x_t(i-1)) + F(x_t(i+1))] + \eta_t, \quad (1)$$

where $x_t(i)$, $i = 1, 2, \dots, L$, is value of the variable located at site i at time t , η_t is the additive noise, ε is the (nearest neighbor) coupling strength, and L is the size of the lattice.

Evolution on the lattice sites is governed by the nonlinear logistic function

$$F(x) = \mu x(1 - x), \quad (2)$$

where μ is the nonlinearity parameter. Both open-boundary conditions $x_t(0) = x_t(1)$, $x_t(L+1) = x_t(L)$, and periodic-boundary conditions $x_t(L+i) = x_t(i)$, have been used for our system. For noise η_t we have chosen a uniformly distributed random number bounded between $-W$ and $+W$. We call W the *noise-strength* parameter.

We define a *structure* as a region of space such that the dynamical variables at sites within this region follow a prespecified spatial pattern [13]. For our purpose we choose a spatial pattern where the difference in the values of the variables of neighboring sites within the structure is less than a predefined small positive number say δ , i.e.,

$$|x_t(i) - x_t(i \pm 1)| \leq \delta .$$

We call δ the *structure parameter*. We study the distributions of abundance and lifetimes of these coherent structures as the CML evolves chaotically.

III. RESULTS AND DISCUSSION

Values of the system parameters μ , ε and L are so chosen that the dynamics of the system remains essentially chaotic. We have taken typical values $L = 10000$, $\mu = 4$ and $\varepsilon = 0.6$. Value of structure parameter δ is chosen as $\delta = 0.0001$. Coherent structures with length < 3 (sites) and lifetime < 2 (timesteps) are disregarded. W is restricted to within $[0, 1]$. For the results presented here open-boundary conditions are used. 80000 transient steps have been discarded and the data are integrated over 100000 iterates per initial condition and 4 different initial conditions.

A. Distribution of $n(l)$ vs. l

We have investigated the distribution of number $n(l)$ of structures with their length l , for different values of noise-strength parameter W . In Fig. 1 we show the plot (on log-log scale) of $n(l)$ against l , for five values of W . The plot exhibits, over a wide range of scales, a characteristic *power-law* of the form

$$n(l) \propto l^{-\alpha_1} , \quad (3)$$

where α_1 is power-law exponent.

If one uses only a uniform-deviate random number as site-variable, probability that a site belongs to a structure of length l is $p_\delta(l) \approx l(2\delta)^{l-1}(1-2\delta)^2$. So the number of such structures in a lattice of size L will be

$$n_\delta(l) \approx L(2\delta)^{l-1}(1-2\delta)^2 , \quad (4)$$

which shows an exponential decay. Thus correlations in the system are important to get a power law form.

B. Stochastic coherence

One can see from Fig. 1 that the exponent α_1 of relation (3) depends on noise-strength W . Fig. 2 shows the variation of α_1 with W . α_1 is exhibiting a minimum for values of W around 0.6. To get a clearer picture, let us define average length \bar{l} of a structure as

$$\bar{l} = \sum l n(l) / \sum n(l). \quad (5)$$

We have investigated how noise influences this quantity. In Fig. 3 we plot the variation of \bar{l} with W for values of parameters as in Fig. 1. One sees a quite interesting *bell-shaped* dependence for W around value 0.6.

This behavior may remind one of the much studied stochastic resonance phenomenon [28–30], a signature of which is the existence of a bell-shaped behavior of the temporal response of the system, when plotted against noise-strength. The similarity, however, is purely coincidental because there exists one important difference. In stochastic resonance noise transfers energy to the system at a given time scale, which usually is the characteristic scale of the system. On the other hand, power law feature of Fig. 1 implies that our system does not have any preferred length scale; noise *induces coherence* on all length scales. We call this novel phenomenon *stochastic coherence*.

C. Stability analysis

Let us see, qualitatively, how noise modifies the stability matrix of the system, thereby influencing its stability properties. We consider stability matrix M of a homogeneous state $\{\dots, x_t, x_t, x_t, \dots\}$ at time t . This state may be imagined as a large structure with $\delta = 0$. One time step later the stability matrix is

$$M_{t+1} = JF'_t, \quad (6)$$

where J is the familiar tridiagonal matrix

$$J = \begin{pmatrix} \ddots & & & & \\ & \ddots & & & \\ & & 1 - \varepsilon & \varepsilon/2 & 0 \\ & & \varepsilon/2 & 1 - \varepsilon & \varepsilon/2 \\ & & 0 & \varepsilon/2 & 1 - \varepsilon & \ddots \\ & & & & & \ddots & \ddots \end{pmatrix} \quad (7)$$

with $1 - \varepsilon$ as its diagonal elements and $\varepsilon/2$ as offdiagonal elements on either sides, and

$$F'_t \equiv F'(x_t) (\equiv \frac{dF}{dx}) = \mu(1 - 2x_t). \quad (8)$$

After two more timesteps, the stability matrix takes the form

$$\begin{aligned} M_{t+1}M_{t+2}M_{t+3} &= J^3 F'_t F'_{t+1} F'_{t+2} \\ &= J^3 F'_t \mu^2 [(1 - 2F_t) \{1 - 2\mu F_t(1 - F_t)\} + 6\mu \eta_t^2 (1 - 2F_t) \\ &\quad - 2\eta_t \{1 + \mu(1 - 6F_t + 6F_t^2)\} - 4\mu \eta_t^3 - 2\eta_{t+1}(1 - 2F_t) + 4\eta_t \eta_{t+1}]. \end{aligned}$$

We now average this expression over the noise distribution. The noise has uniform distribution, with zero mean and delta-correlation. By averaging, the terms containing cross terms in η (i.e. terms of the type $\eta_t \eta_{t+1}$) and odd powers in η vanish, leaving the following expression with only even powers in η :

$$\langle M_{t+1}M_{t+2}M_{t+3} \rangle = J^3 (F'_t)^2 \mu [1 - 2\mu F_t(1 - F_t) + 6\mu \langle \eta_t^2 \rangle], \quad (9)$$

where $\langle \rangle$ denotes averaging over noise-distribution. One more averaging is needed, this time over the invariant distribution of the CML. Fig. 4 shows the invariant density of a

single site of CML, with $W = 0.6$ and the other system parameters same as mentioned in the beginning of this section. The density is highly asymmetric, with larger weightage for $x(i) > 0.5$. Because of this asymmetry, averaging expression (9) over the invariant density makes the term $1 - 2\mu F_t(1 - F_t)$ negative. This, added to the positive noise term $6\mu < \eta_t^2 >$, results in reduction of eigenvalue of the above matrix. This in turn implies a consequent reduction of the instability of the state (or the structure). Thus noise plays a crucial role in enhancing the abundance of the structures.

D. Evolution of structures

Let us now consider the evolutionary aspects of these coherent structures. We have studied the distribution of the number $n(\tau)$ of structures having lifetime τ . In order to obtain τ , each structure is tracked as the lattice evolves, till the structure degenerates completely. In Fig. 5 we show such an evolutionary diagram for a CML with a typical size $L = 100$, evolving chaotically for 200 timesteps. The shaded regions depict the evolution of coherent structures. Fig. 6 shows the variation, on log-linear scale, of $n(\tau)$ with τ , for different values of noise W . Number $n(\tau)$ exhibits a decay with τ with a *stretched exponential* form

$$n(\tau) \propto \exp(-(\text{const.})\tau^\beta). \quad (10)$$

The exponent β is seen to depend on W . Like in case of α of expression (3), β also exhibits a minimum near $W = 0.6$.

We define average lifetime $\bar{\tau}$ of a structure as

$$\bar{\tau} = \sum \tau n(\tau) / \sum n(\tau), \quad (11)$$

and explore its dependence on noise strength W . Fig. 7 shows a plot of $\bar{\tau}$ vs. W . It again exhibits a maximum for W around 0.6.

There is another feature of the system which merits an elaborate study. This concerns the distribution of ‘spatio-temporal structures (STS)’. By such a structure we mean the group of sites that remain in a coherent structure as it evolves in time, till it completely degenerates. Each shaded region of Fig. 5 constitutes one such STS. In Fig. 8 we plot the number $n(S_1)$ of an STS vs. its ‘size’ S_1 for different noise values W . We again see an

interesting power law dependence of the type (3) for an appreciable range of sizes, but with different exponent. This exponent also depends on W , with a minimum around $W = 0.6$. Let us define average size \bar{S}_1 of an STS in a similar fashion as

$$\bar{S}_1 = \sum S_1 n(S_1) / \sum n(S_1). \quad (12)$$

We plot \bar{S}_1 as function of W in Fig. 9. This plot also exhibits a characteristic bell shape within a range around $W = 0.6$, quite similar to the plot in Fig. 3.

E. Lyapunov spectrum analysis

We have studied the lyapunov exponent spectrum (λ spectrum) of the CML, and its dependence on noise W as well as on the coupling parameter ε . We find that a number of lyapunov exponents is positive, thereby implying that the system is indeed evolving chaotically. In Fig. 10 we plot the variation of maximum exponent λ_{\max} with noise strength W , for coupling parameter $\varepsilon = 0.6$. λ_{\max} exhibits a clear minimum around $W = 0.6$ [31], the same region where all the extrema reported above are located. This observation may create the impression that the reduction of lyapunov exponent alone is responsible for stochastic coherence.

To explore this possibility, we have studied the dependence of both λ_{\max} and average length \bar{l} on coupling strength ε . Fig. 11 plots the variation of λ_{\max} with ε for different W . It is clear that λ_{\max} remains fairly constant for $0.2 \leq \varepsilon \leq 0.8$ for all W . On the other hand, \bar{l} shows a monotonic increase with ε for all W . In Fig. 12 we show one such plot of \bar{l} against ε , for $W = 0.6$. These two contrary features indicate that lyapunov exponent alone is not good enough to characterize the full range of spatio-temporal features of the system.

It is worth pointing out that stochastic coherence is quite distinctive phenomenon as compared to spatio-temporal intermittency [32]. In intermittency the system exhibits alternately regular and chaotic bursts in time. Our system does not show any such behavior. This fact is further corroborated by the fact that the power spectrum of time-series does not have any peak for entire range of noise-strength. Thus our system is undergoing essentially a *spatially intermittent and temporally chaotic* evolution.

F. Full lattice coherence (FLC)

One quite interesting phenomenon that we have observed is that for $W \geq 0.4$ often the entire lattice itself evolves as a single coherent structure. This state should be distinguished from the synchronized state where at any given instant t , $x_t(i) = x_t$ for $i = 1, 2, \dots, L$ (that is, $\delta = 0$). On occasions this *full lattice coherence* (FLC) survives for quite long durations (as long as 200 timesteps or more), but eventually degenerates completely. This implies that synchronized state is not a stable attractor for our system. We have confirmed this by calculating the largest Lyapunov exponent for the synchronized state which turns out to be positive.

However, occasionally our system did fall into an apparently synchronized state after a very large time (larger than 10^7 steps). This happens because of finite accuracy of computation which cannot differentiate between unstable and stable synchronized states [33]. Let us investigate this point further. We define a quantity \bar{T} as the average time required for first occurrence of FLC, the averaging taken over different initial conditions. In Fig. 13 we plot, on log-log scale, \bar{T} against the structure parameter δ , for a fixed lattice size $L = 10000$. The plot exhibits a power law of the form

$$\bar{T}_L \propto \delta^{-\gamma} . \quad (13)$$

This relation implies that the synchronized state ($\delta = 0$) will not occur in a finite lattice. We now show, in Fig. 14, the plot of \bar{T} against lattice size L , for a fixed δ . This is again a power law of the type

$$\bar{T}_\delta \propto L^\nu . \quad (14)$$

We thus see that as $L \rightarrow \infty$, even FLC with a nonzero δ will not be attained. Therefore, relations (13) and (14) tell us that synchronized state for our system is an artifact, resulting due to the combined effect of finite lattice size and finite computational accuracy.

Existence of FLC in a finite lattice can be seen to be a consequence of the power-law (3). Probability of a site to belong to a structure of length l , following (3), is $p_\delta(l) \propto l.l^{-\alpha_1} = l^{1-\alpha_1}$. The probability of a site to belong to a structure of length $\geq L$ is then $P_0 \equiv P_\delta(\geq L) \propto \sum_L^\infty l^{1-\alpha_1} \approx \int_L^\infty dl l^{1-\alpha_1} \propto L^{2-\alpha_1}$ (this holds for $\alpha_1 > 2$, which is true for

our system as can be seen from Fig. 2). Thus, the probability that for the first time a site belongs to a structure of length $\geq L$ at timestep T is $P_\delta(T) \propto (1 - P_0)^{T-1} P_0$. Average of T is $\bar{T}_\delta(\geq L) = \sum_{T=1}^{\infty} T P_\delta(T) \propto (P_0)^{-1}$, i.e.,

$$\bar{T}_\delta(\geq L) \propto L^{\alpha_1 - 2} . \quad (15)$$

This shows that FLC (with nonzero δ) will occur in a finite lattice. From Fig. 2 we get $\alpha_1 - 2 \approx 0.22$ for $W = 0.6$. On the other hand, we estimate (from Fig. 14) ν of relation (14) to be approximately 0.3. The discrepancy may occur due to the fact that relation (15) holds for an infinite lattice, whereas relation (14) is numerically obtained for finite lattices.

IV. TWO DIMENSIONAL CML

Let us now consider a two dimensional CML. The dynamics of this system takes the form

$$x_{t+1}(i, j) = (1 - \varepsilon)F(x_t(i, j)) + \frac{\varepsilon}{4} \left[F(x_t(i - 1, j)) + F(x_t(i + 1, j)) + F(x_t(i, j - 1)) + F(x_t(i, j + 1)) \right] + \eta_t , \quad (16)$$

where $x_t(i, j)$, $i, j = 1, 2, \dots, L$, is the value of the variable at site (i, j) in the lattice having size $L \times L$, and $F(x(i, j)) = \mu x(i, j)(1 - x(i, j))$. For structures in this lattice we look for those sites (i, j) with

$$|x_t(i, j) - x_t(i \pm 1, j)| \leq \delta ,$$

and,

$$|x_t(i, j) - x_t(i, j \pm 1)| \leq \delta .$$

As the CML evolves, we study the distributions of abundance and lifetimes of these two dimensional structures, as we have done for one dimensional system.

We present some of the observations in the following. Again we have chosen the system parameters so that the CML evolves chaotically. Typical values taken are $L \times L = 100 \times 100$, $\mu = 4$, and $\varepsilon = 0.6$. We have chosen structure parameter $\delta = 0.0001$. 3000 transient steps

have been discarded, and data are obtained over 20000 iterates per initial condition and 4 initial conditions. We have used open boundary conditions for the results presented here.

Fig. 15 exhibits the plot (on log–log scale) of distribution of the number $n(s)$ of coherent structures against their size s for different W (we use the notation s to denote size of the structures in two dimensional CML, unlike l which has been used for one dimensional case. This is also to be distinguished from S_1 , the notation used for sizes of STS). One can see a power law of the form

$$n(s) \propto s^{-\alpha_2} , \quad (17)$$

similar to the relation (3), for a wide range of values of s (for $s \geq 10$; there is a slight bend in the graphs for $s \leq 10$). The exponent α_2 for the power law is slightly less in value than its one dimensional counterpart α_1 , for all W , indicating a less steeper decay. These exponents again show a dip around $W = 0.6$. We define the average size \bar{s} of the structures as

$$\bar{s} = \sum s n(s) / \sum n(s) . \quad (18)$$

\bar{s} exhibits a corresponding peak around $W = 0.6$. This can be clearly seen in the bell–shaped curve of Fig. 16, which is the plot of \bar{s} against W . This plot is quite alike the one of Fig. 3.

In Fig. 17 we plot, on log–linear scale, distribution of number $n(\tau)$ of structures against their lifetime τ . The plot shows a stretched exponential type behavior of the form (10), similar to Fig. 6. Fig. 18 shows the variation of average lifetime $\bar{\tau}$, as defined in (11), with noise strength W . We see a peak near $W = 0.6$, quite similar to the plot of Fig. 7.

Distribution of number $n(S_2)$ of STS is plotted, on log–log scale, against size S_2 in Fig. 19. We see a very similar power law decay as in Fig. 8 for one dimensional CML. As in previous instances, we define average size \bar{S}_2 of STS as

$$\bar{S}_2 = \sum S_2 n(S_2) / \sum n(S_2). \quad (19)$$

Fig. 20 shows the variation of \bar{S}_2 with noise strength W . The plot shows a bell–shaped peak around $W = 0.6$, similar to the plot of Fig. 9.

All the other features that are observed in one dimensional system are also seen in two dimensional CML. For instance, we have seen full lattice coherence for $W \geq 4$, which persist for considerable duration before eventually breaking up.

We have repeated all the above observations, for both one and two dimensional systems, for several other values of the coupling parameter ε ranging from 0.1 to 0.9, as well as for nonlinearity parameter μ between 3.6 and 4. We find that all the features remain essentially the same, indicating the robustness of the phenomenon. We have also observed similar results using periodic–boundary conditions for the lattice.

V. CONCLUSION

We have investigated in details a new phenomenon associated with structures in a chaotically evolving CML, in both one and two dimensions, driven by identical noise. We call this phenomenon *stochastic coherence*. We have seen a marked rise in abundance of coherent structures of all scales due to noise. Stability matrix of these structures shows that noise can reduce their instability, thereby enhancing abundance.. Distribution of the structures exhibits a power–law decay with size of the structure, with an exponent having a minimum at some intermediate noise–strength. Average size of these structures shows a bell–shaped maximum at the same value of noise–strength. This feature is similar to that of the stochastic resonance phenomenon. However, our system does not have any intrinsic length–scale, whereas stochastic resonance is associated with a given time–scale. We have also observed similar maxima for the average lifetime of these structures as well as for the average size of ‘spatio–temporal structures’, at the value of noise close to the earlier extrema. Our phenomena may have their importance in understanding the interesting role that noise plays in formation and evolution of structures in spatially extended systems.

VI. ACKNOWLEDGEMENTS

One of the authors (MR) acknowledges University Grants Commission (India) and the other (REA) acknowledges Department of Science and Technology (India) for financial assistance.

REFERENCES

- [1] Y. Oono and S. Puri, Phys. Rev. Lett. 58 (1986) 836.
- [2] G.L. Oppo and R. Kapral, Phys. Rev. A 36 (1987) 5820.
- [3] P.M. Gade and R.E. Amritkar, Phys. Rev. E 47 (1993) 143.
- [4] R.E. Amritkar and P.M. Gade, Phys. Rev. Lett. 70 (1993) 3408.
- [5] Theory and applications of coupled map lattices, K. Kaneko, ed. (John Wiley and Sons, England, 1993).
- [6] T. Yanagita and K. Kaneko, Phys. Lett. A 175 (1993) 415.
- [7] Qu Zhilin and Hu Gang, Phys. Rev. E 49 (1994) 1099.
- [8] S. Raghavachari and J.A. Glazier, Phys. Rev. Lett. 74 (1995) 3297.
- [9] S. Sinha, D. Biswas, M. Azam and S.V. Lawande, Phys. Rev. A 46 (1992) 6242.
- [10] J.D. Keeler and J.D. Farmer, Physica D 23 (1986) 413.
- [11] I. Aranson, D. Golomb and H. Sompolinski, Phys. Rev. Lett. 68 (1992) 3495.
- [12] N. Chatterjee and N.M. Gupte, Phys. Rev. E 53 (1996) 4457.
- [13] J.K. John and R.E. Amritkar, Phys. Rev. E 51 (1995) 5103.
- [14] M.C. Cross and P.C. Hohenberg, Rev. Mod. Phys. 65 (1993) 851.
- [15] A. K. M. F. Hussain, Phys. Fluids 26 (1983) 2816.
- [16] Topological Fluid Mechanics, H.K. Moffatt et. al., ed. (proceedings of the IUTAM symposium, Cambridge University Press, 1990).
- [17] Turbulence And Stochastic Processes: Kolmogorov's Ideas 50 Years On, J.C.R. Hunt et. al., ed. (The Royal Society, London, 1991).
- [18] Noise in Dynamical Systems, F. Moss and P.V.E. McClintock, ed. (Cambridge University Press, Cambridge, U.K., 1989).

- [19] P.C. Hohenberg and J.B. Swift, *Phys. Rev. A* 46 (1992) 4773.
- [20] C. Van den Broeck, J.M.R. Parrondo, R. Toral and R. Kawai, *Phys. Rev. E* 55 (1997) 4084.
- [21] X-G Wu and R. Kapral, *J. Chem. Phys.* 100 (1994) 1.
- [22] S. Fahy and D.R. Hamann, *Phys. Rev. Lett.* 69 (1992) 761.
- [23] D.A. Kurtze, *Phys. Rev. Lett.* 77 (1996) 63.
- [24] A. Maritan and J.R. Banavar, *Phys. Rev. Lett.* 72 (1994) 1451.
- [25] P. Jung and G. Mayer-Kress, *Phys. Rev. Lett.* 74 (1995) 2130.
- [26] P.M. Gade and C. Basu, *Phys. Lett. A* 217 (1996) 21.
- [27] M. Roy and R.E. Amritkar, *Phys. Rev. E* 55 (1997) 2422.
- [28] R. Benzi, G. Parisi, A. Suter and A. Vulpiani, *Tellus* 34 (1982) 10.
- [29] B. McNamara, K. Wiesenfeld and R. Roy, *Phys. Rev. Lett.* 60 (1988) 2626.
- [30] R.F. Fox and Yan-nan Lu, *Phys. Rev. E* 48 (1993) 3390.
- [31] K. Matsumoto and I. Tsuda, *J. Stat. Phys.* 31 (1983) 87; 34 (1984) 111.
- [32] H. Chaté and P. Manneville, *Phys. Rev. Lett.* 58 (1987) 112; *Physica D* 32 (1988) 409.
- [33] A. S. Pikovsky, *Phys. Rev. Lett.* 73 (1994) 2931.

FIGURE CAPTIONS

- Fig. 1. The figure shows the variation, on log–log scale, of number $n(l)$ of structures with length l for a one dimensional lattice with size $L = 10000$, for different values of noise–strength W as indicated. The system parameters are coupling strength parameter $\varepsilon = 0.6$, structure parameter $\delta = 0.0001$, and nonlinearity parameter $\mu = 4$. Open–boundary conditions are used. 80000 transient steps are discarded. Data are obtained for 100000 iterates per initial condition and with 4 initial conditions.
- Fig. 2. Exponent α_1 of the power law (3) (slope of the plots in Fig. 1) is plotted against noise strength W , with system parameters as in Fig. 1.
- Fig. 3. Variation of average length \bar{l} of structure with W is plotted, with parameters as stated in Fig. 1. Vertical error bars indicate the standard deviations at the data points.
- Fig. 4. Invariant density $p(x)$ of the CML is plotted against variable value x , for the system parameters as for Fig. 1 and with noise value $W = 0.6$. The asymmetry is clearly evident, with a much higher weightage for $x > 0.5$.
- Fig. 5. Evolution of coherent structures is shown by shaded regions, during 200 time steps, in a CML with a typical size $L = 100$, and with noise value $W = 0.6$, and other parameters same as in earlier figures.
- Fig. 6. Distribution of number $n(\tau)$ of the structures is plotted, on log–linear scale, against their lifetime τ . The system parameters are as in Fig. 1.
- Fig. 7. Plot shows the variation of average lifetime $\bar{\tau}$ of structures with noise–strength W , for parameters as in Fig. 1.
- Fig. 8. Distribution of the number $n(S_1)$ of spatio–temporal structures (STS) is plotted, on log–log scale, against their size S_1 , for the same parameter values as in Fig. 1.
- Fig. 9. The plot shows the variation of average size \bar{S}_1 of STS with the noise–strength W , for parameter values as in earlier figures.

Fig. 10. Variation of λ_{\max} is plotted against noise strength W , for $\varepsilon = 0.6$.

Fig. 11. The plot shows variation of λ_{\max} with coupling strength ε , for different values of W , other system parameters remaining the same as in Fig. 1.

Fig. 12. Average length \bar{l} of the structures is plotted against ε , for $W = 0.6$.

Fig. 13. Variation of \bar{T} is plotted, on log–log scale, against δ , for given lattice size $L = 10000$, other parameters being as in earlier figures.

Fig. 14. The plot shows, on log–log scale, the variation of \bar{T} with lattice size L , for given structure parameter $\delta = 0.0001$.

Fig. 15. Number $n(s)$ of structures is plotted, on log–log scale, against their size s , for two dimensional lattice with size $L \times L = 100 \times 100$, for different W . Parameters taken are $\varepsilon = 0.6$, $\mu = 4$, and $\delta = 0.0001$. We have used open–boundary conditions. 3000 transients are discarded. Data are obtained for 20000 iterates per initial conditions and with 4 initial conditions.

Fig. 16. The plot shows variation of average size \bar{s} of the two dimensional structures with noise W , for the parameters as stated in Fig. 15. Error bars indicate the standard deviations at the data points.

Fig. 17. Distribution of $n(\tau)$ is plotted for two dimensional CML, on log–linear scale, against the lifetime τ of the structures, for system parameters as in Fig. 15.

Fig. 18. Plot shows variation of τ with noise W , for two dimensional CML.

Fig. 19. Distribution of the number $n(S_2)$ of STS is plotted, on log–log scale, against the size S_2 , for different noise strength values W , for a two dimensional CML, parameters being same as in Fig. 15.

Fig. 20. Variation of average size \bar{S}_2 is shown against noise strength value W for a two dimensional CML.

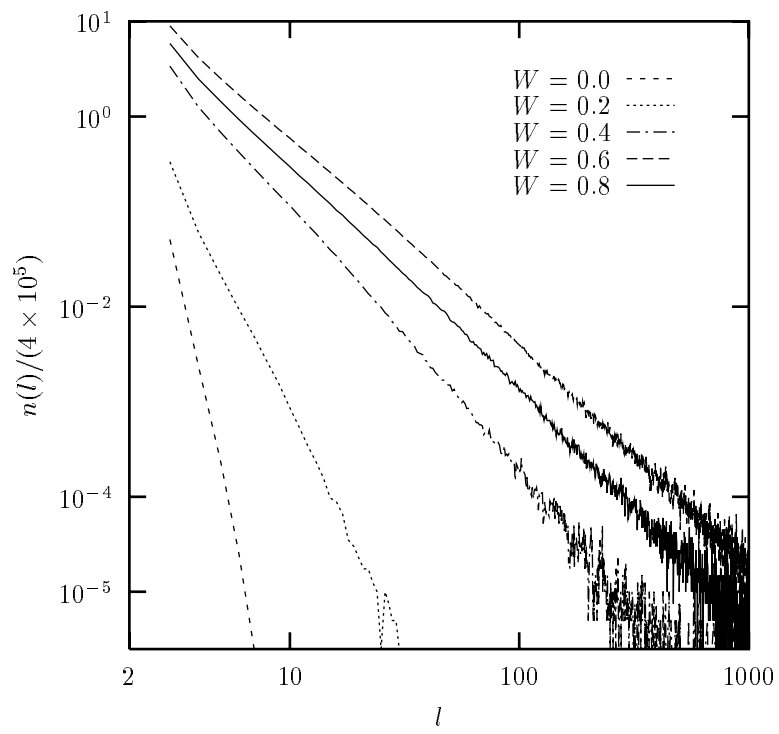


Fig. 1

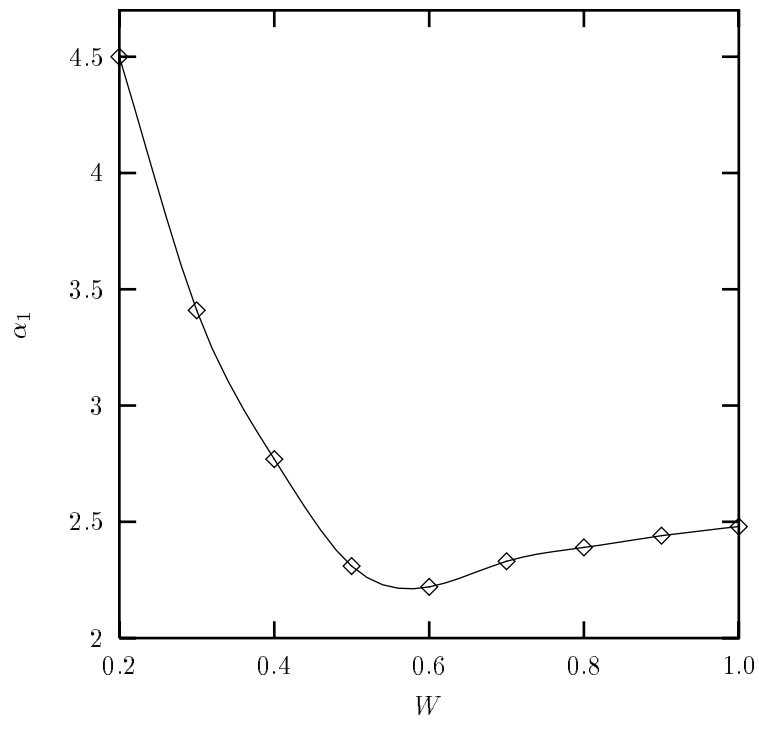


Fig. 2

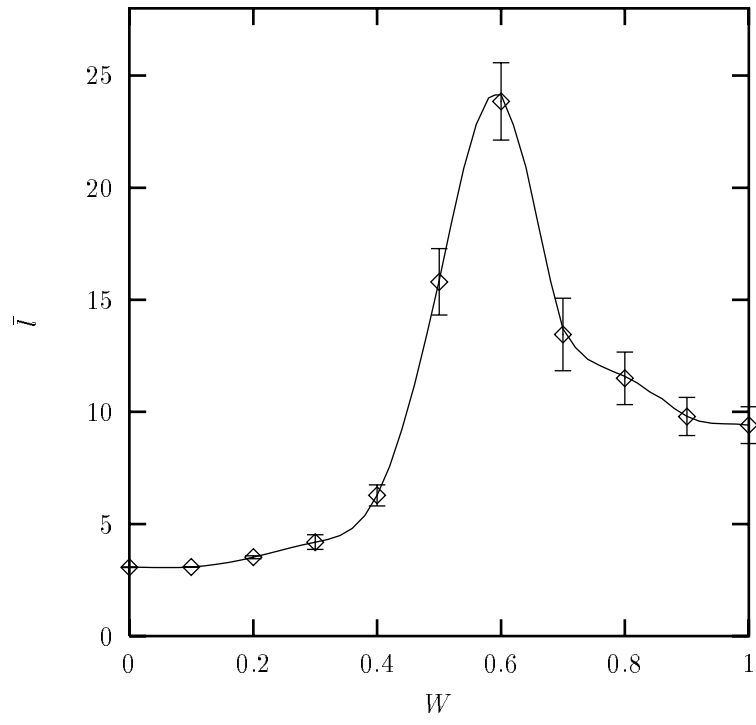


Fig. 3

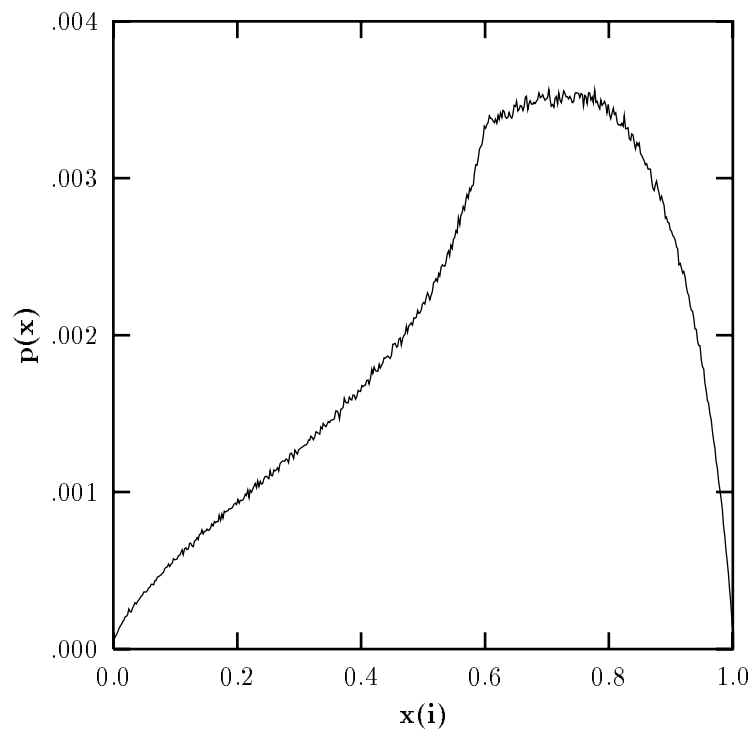


Fig. 4

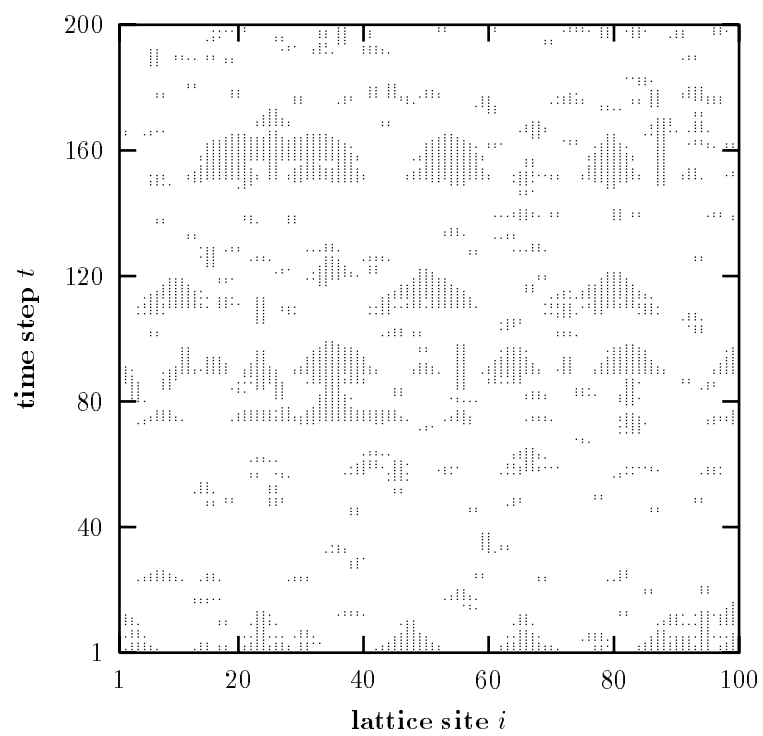


Fig. 5

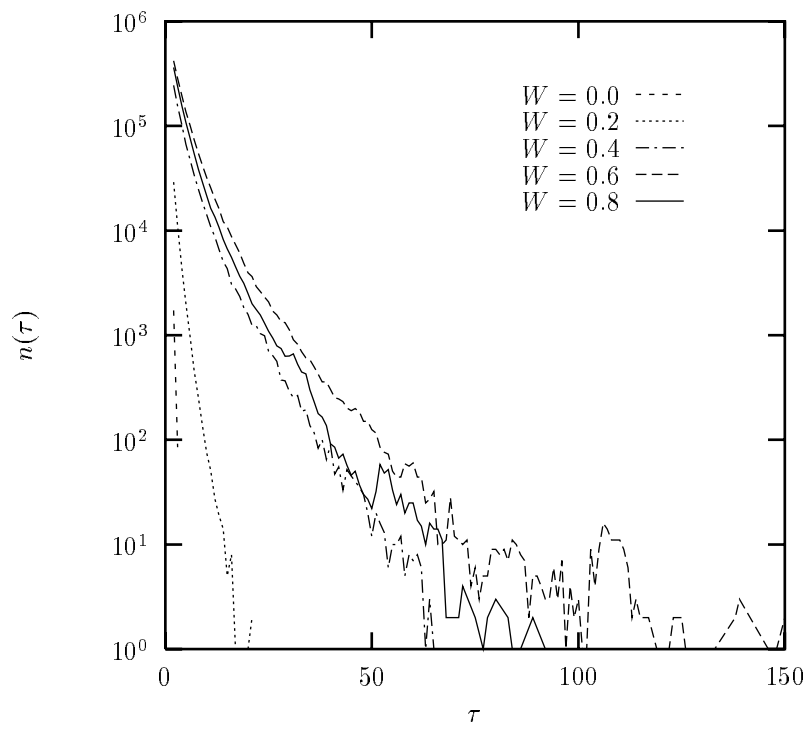


Fig. 6

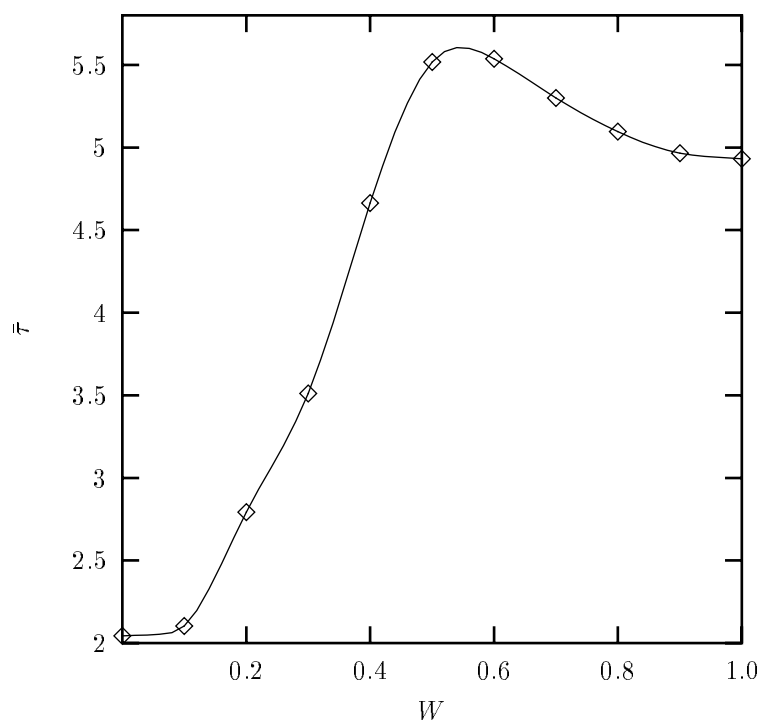


Fig. 7

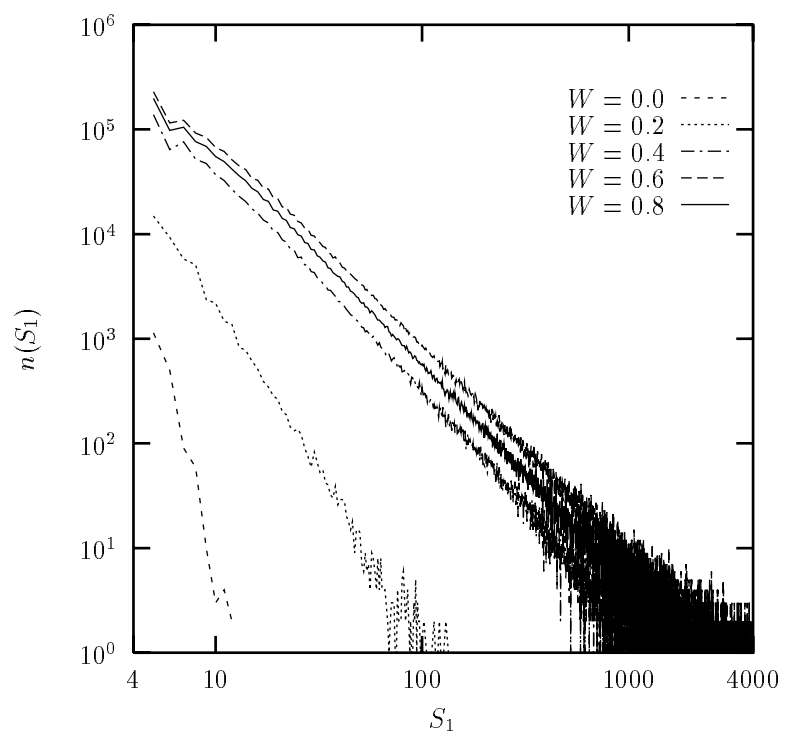


Fig. 8

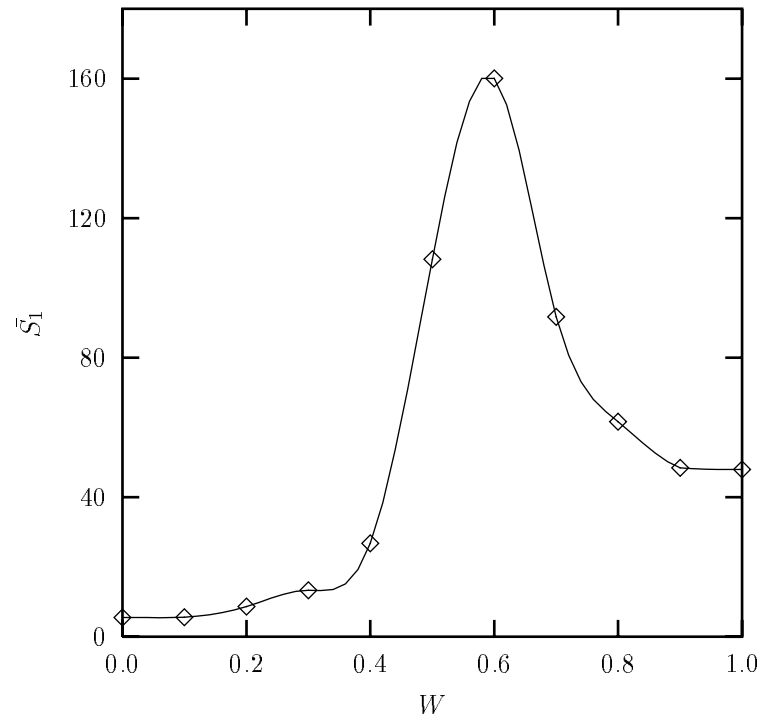


Fig. 9

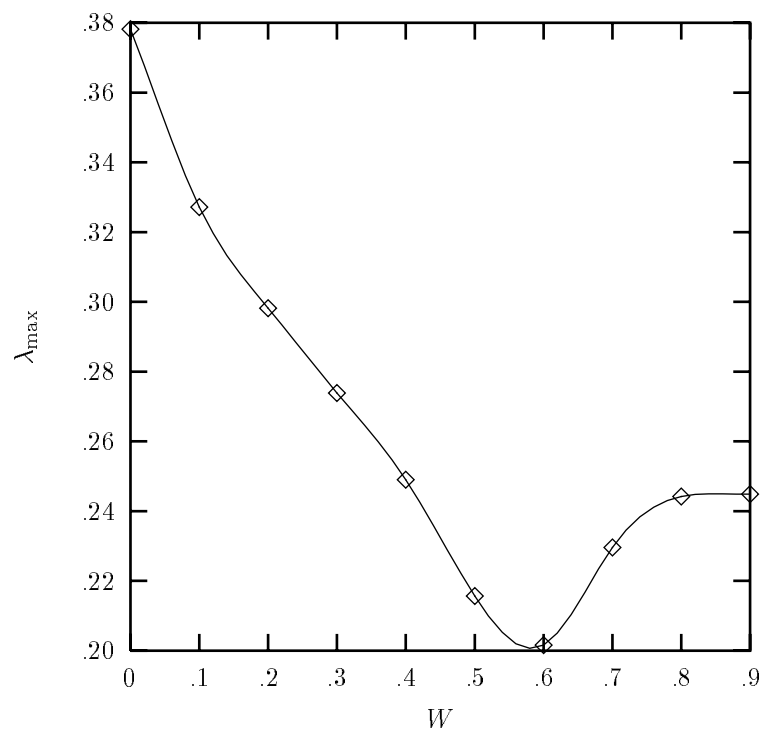


Fig. 10

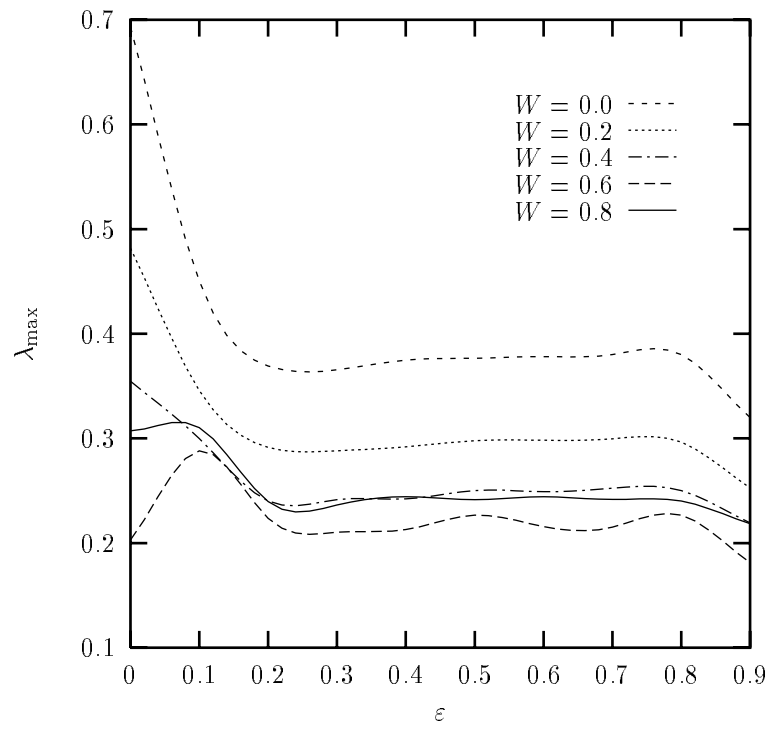


Fig 11

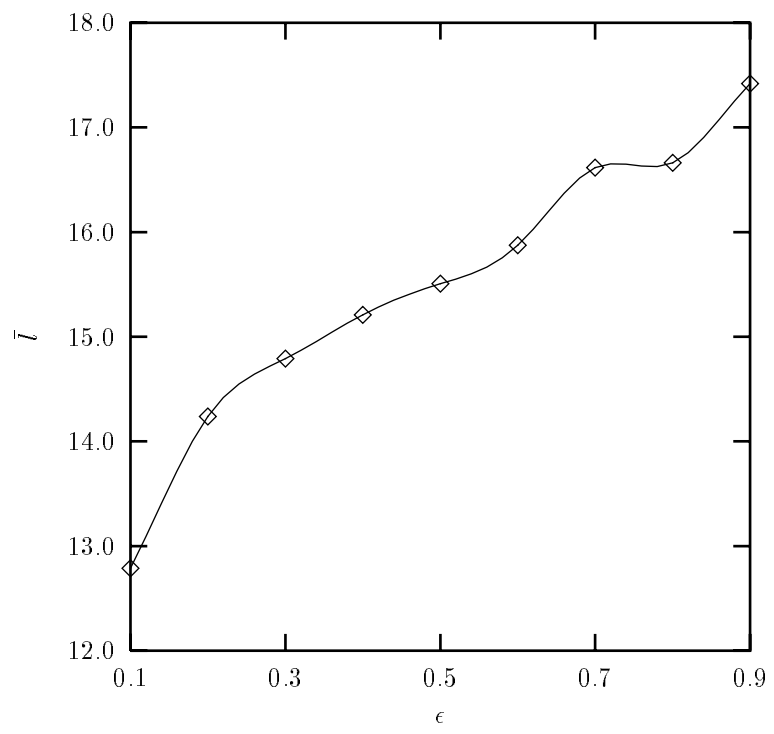


Fig. 12

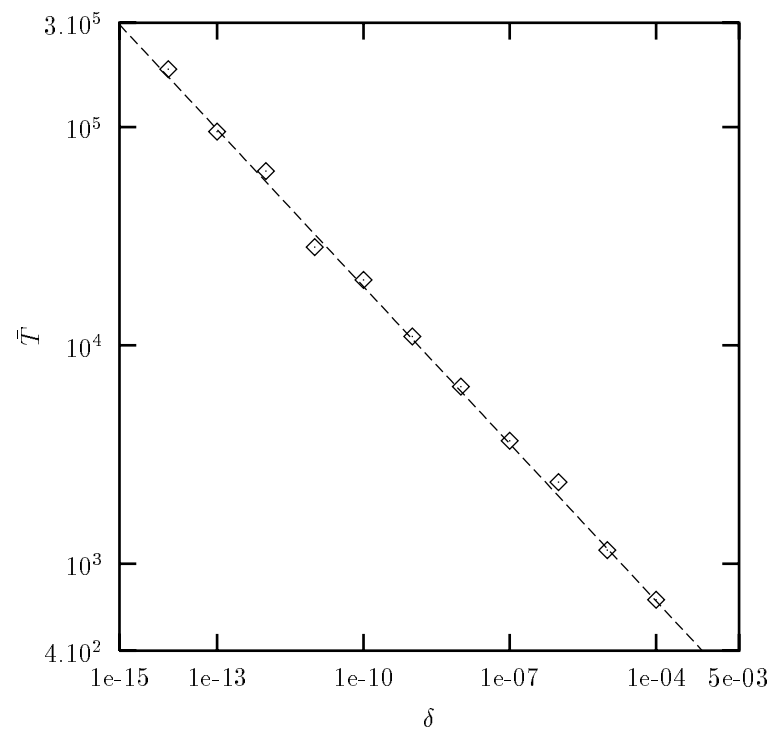


Fig. 13

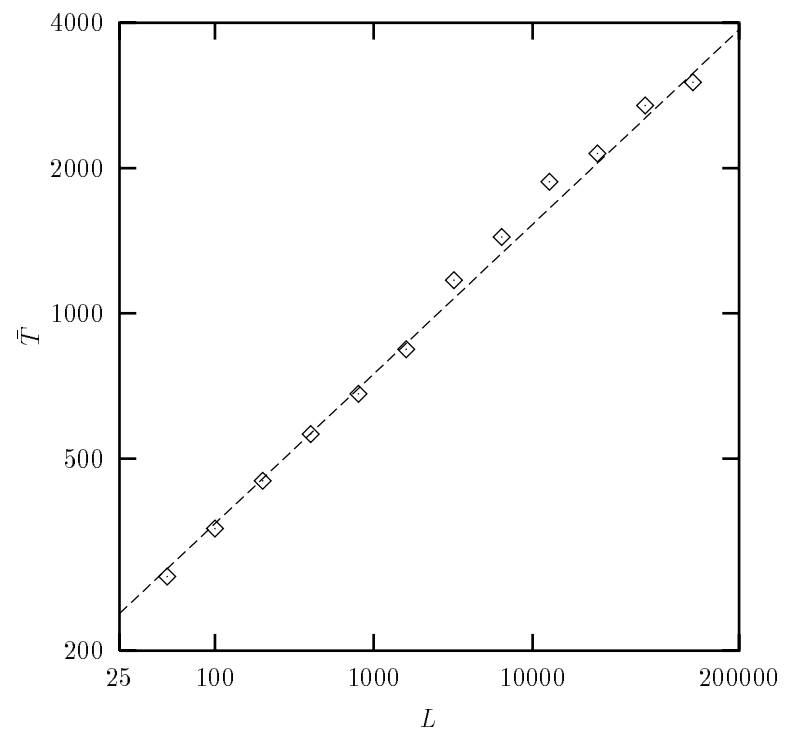


Fig. 14

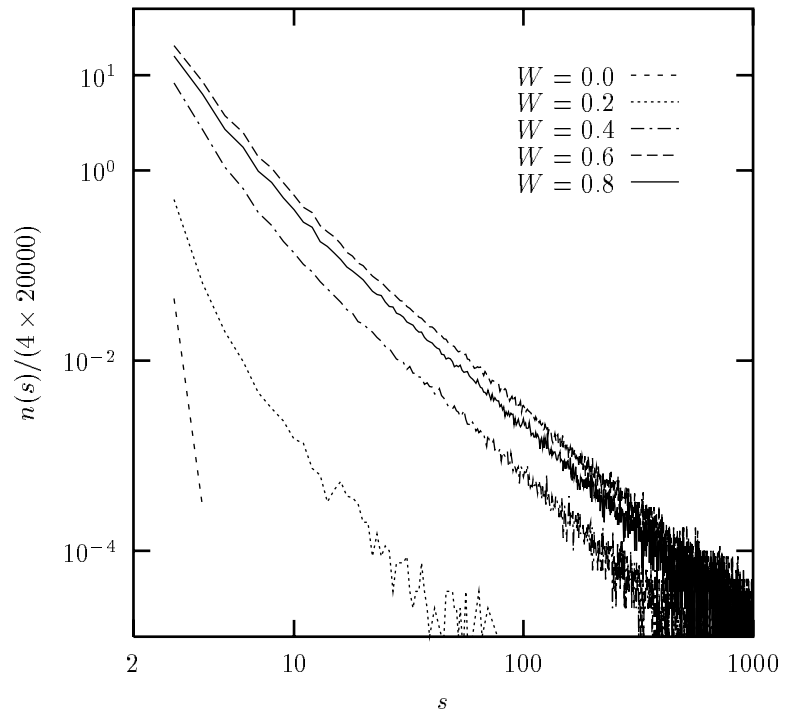


Fig. 15

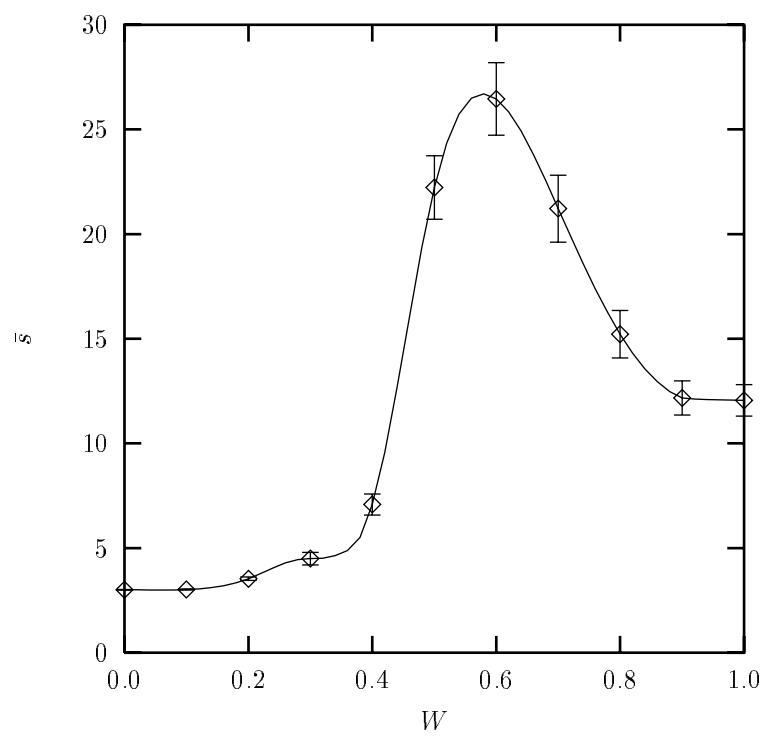


Fig. 16

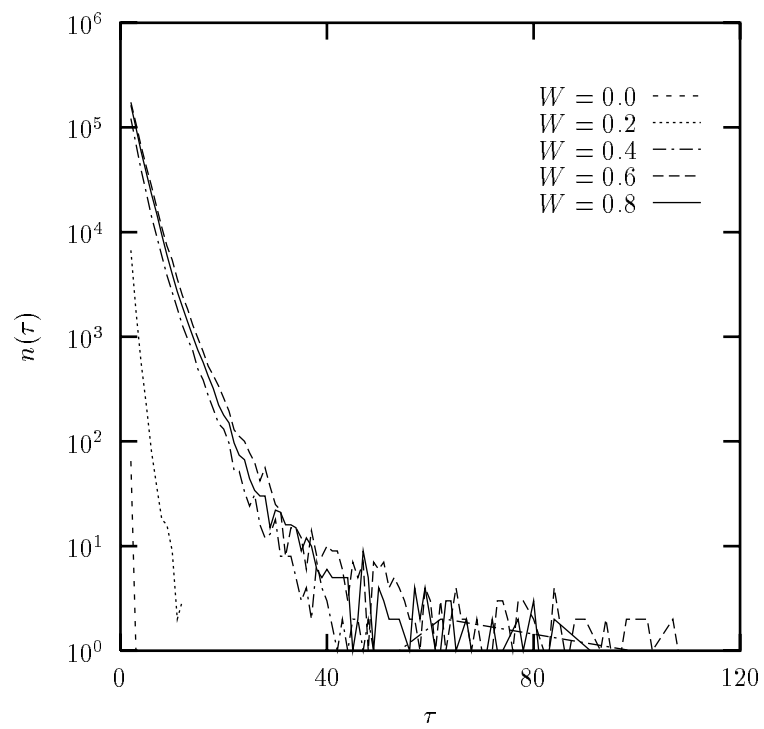


Fig. 17

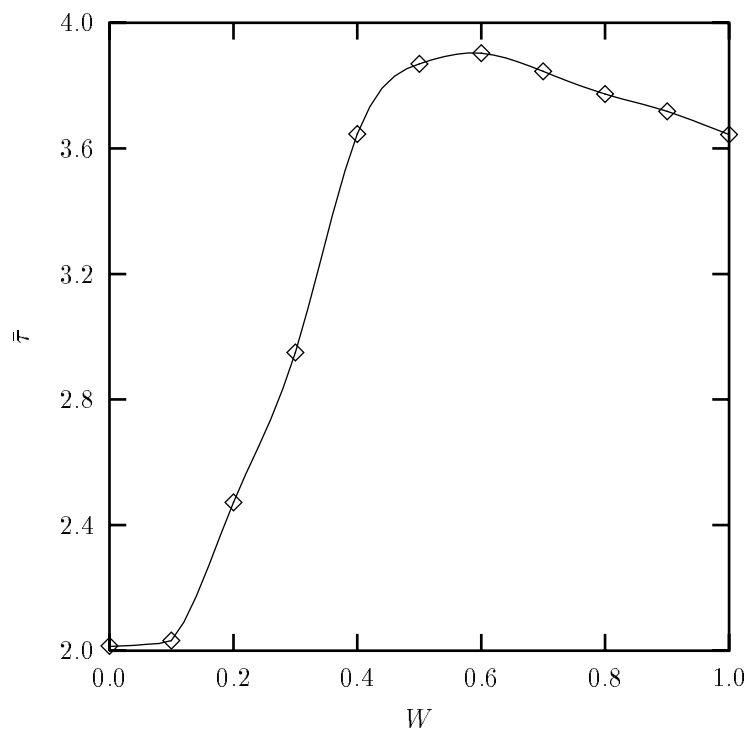


Fig. 18

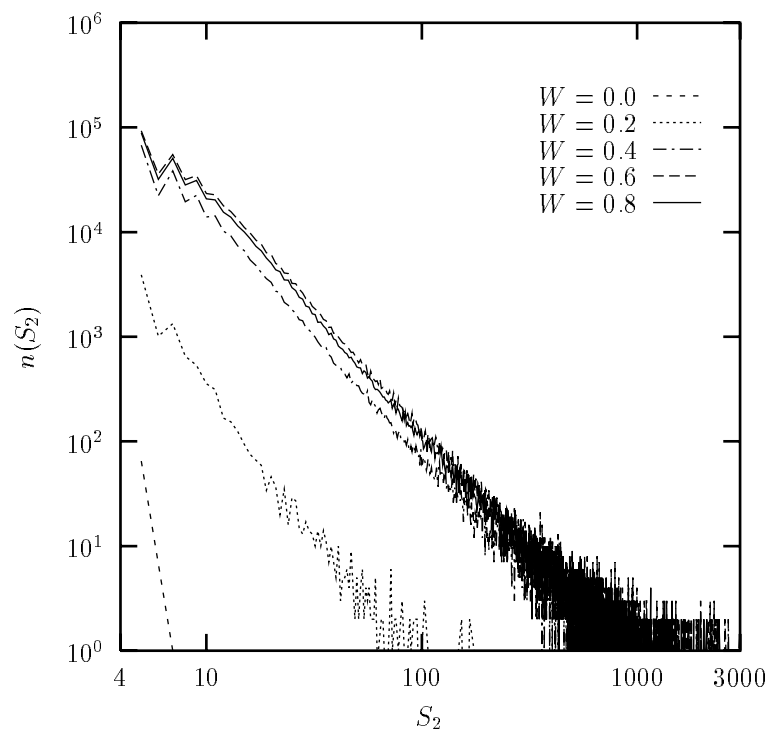


Fig. 19

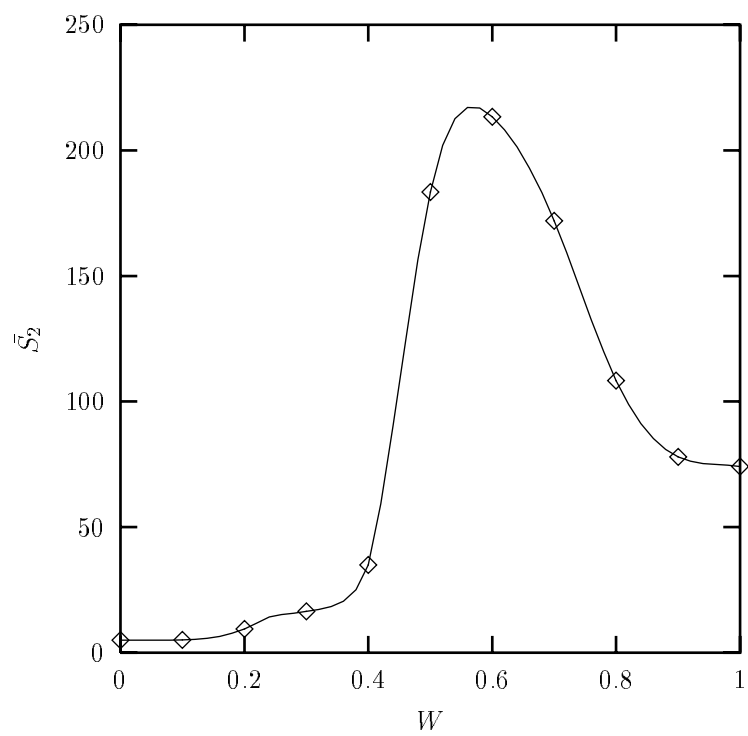


Fig. 20